Journal of Alloys and Compounds 480 (2009) 386–391

Contents lists available at ScienceDirect

Journal of Alloys and Compounds

journal homepage: www.elsevier.com/locate/jallcom

Influence of flux containing YCl_3 additions on purifying effectiveness and properties of Mg–10Gd–3Y–0.5Zr alloy

Wei Wang[a,b], Yuguang Huang[a,b], Guohua Wu[a,b,*], Qudong Wang[a,b], Ming Sun[a,b], Wenjiang Ding[a,b]

[a] National Engineering Research Center of Light Alloy Net Forming, Shanghai Jiao Tong University, Shanghai 200240, China
[b] State Key Laboratory of Metal Matrix Composites, Shanghai Jiao Tong University, Shanghai 200240, China

ARTICLE INFO

Article history:
Received 18 January 2009
Received in revised form 13 February 2009
Accepted 17 February 2009
Available online 3 March 2009

Keywords:
Metals
Rare earth elements and compounds
Mechanical properties
Corrosion
Thermodynamic properties

ABSTRACT

In order to improve the purifying efficiency of RJ6 flux, 5 wt.% YCl_3 additions were introduced into the flux to refine Mg–10Gd–3Y–0.5Zr (GW103K) alloy. The results show that the RJ6 flux containing 5 wt.% YCl_3 additions exhibits excellent adsorption ability to nonmetallic inclusions. Thermodynamic analysis indicates that the main reason could be attributed to the decrease of the surface tension of the flux. Moreover, the mechanical, corrosion and fluidity properties of the alloy were investigated. It was found that these properties were improved to a certain degree due to the removal of nonmetallic inclusions in the alloy.

1. Introduction

Magnesium alloys containing heavy rare earth elements are becoming more and more attractive due to their high strength and ductility. Hence, these alloys show great application prospect in automotive, aircraft and aerospace industries and interest in their application is till increasing. It has been reported that the currently developed Mg–Gd–Y alloys exhibit high specific strength at both room and elevated temperature, and better creep resistance than other Mg-rare earth (RE) alloy such as WE54 [1–8].

Due to their high chemical activities, however, magnesium and rare earth elements tend to oxidize rapidly while smelting. These oxide inclusions destroy the continuity of the magnesium matrix, induce pores and cracks defects, and then impair the mechanical, corrosion and fluidity properties of the alloy [9,10]. Therefore, it is necessary to remove these nonmetallic inclusions from the alloy. Traditional flux refining process is always considered as one of the most effective purifying method because of high efficiency, low cost and easy to operate. $MgCl_2$ is widely accepted as one of the main ingredients in flux because liquid $MgCl_2$ has an excellent adsorption capability to MgO inclusions and forms $MgCl_2{\cdot}5MgO$ compound which sinks to the bottom of the crucible. For Mg–Gd–Y alloys, however, the expensive heavy RE elements Gd and Y tend to react with $MgCl_2$ and they are lost during the refining process. Therefore, the flux without $MgCl_2$, such as RJ6 flux, was engaged to purify RE containing magnesium alloys. Unfortunately, the purifying effectiveness is not as good as the one containing $MgCl_2$ [11]. The lack of efficient purification method becomes a bottleneck which limits the application of GW103K alloy currently.

In this work, in order to improve the purifying ability, 5 wt.% YCl_3 was introduced into RJ6 flux. The surface tensions of the fluxes used in the experiment were determined and its purification mechanism was investigated by thermodynamic calculation. The mechanical, corrosion and fluidity properties of GW103K alloy refined with RJ6 + 5 wt.% YCl_3 additions were investigated as well.

2. Experimental procedure

Pure YCl_3 was added into RJ6 flux and mixed in QM-ISP pebble mill for 3 h. The ingredients of RJ6 containing 5 wt.% YCl_3 are listed in Table 1. GW103K alloy was fabricated by pure Mg ingots and Mg–Gd, Mg–Y, Mg–Zr master alloys. Smelting was performed in a 7 kW crucible electric resistance furnace under protection of a shield gas consisting of SF_6 (1 vol.%) and CO_2 (bal.). 2.5 wt.% (ratio to the whole raw metal) new fluxes were added to refine the melt at 760 °C. After refining, the melt was held for 30–45 min, and then, at 740 °C, poured into the metallic molds preheated to 400 °C.

Tensile tests were conducted on a Zwick/Roell electronic universal material testing machine. For the specimens tested in T6 condition, the T6 heat treatment method was: solution treatment at 500 °C for 8 h in argon atmosphere, peak-ageing at 225 °C in an oil bath for 16 h. The Rigaku Dmax-rc X-ray diffractometer and PHILIPS SEM 515 were employed to analyze phase composition and corrosion morphology, respectively. The composition of inclusions were analyzed by energy dispersive spectroscope (EDS) attached to SEM.

* Corresponding author at: National Engineering Research Center of Light Alloy Net Forming, Shanghai Jiao Tong University, Shanghai 200240, China.
Tel.: +86 21 54742630; fax: +86 21 34202794.
E-mail addresses: ghwu@sjtu.edu.cn, scneu@126.com (G. Wu).

0925-8388/$ – see front matter © 2009 Elsevier B.V. All rights reserved.
doi:10.1016/j.jallcom.2009.02.073

Table 1
Ingredients of the RJ6 + 5 wt.% YCl_3 flux (mass %).

Ingredients	KCl	$BaCl_2$	NaCl	$CaCl_2$	NaCl + $CaCl_2$	H_2O	YCl_3	Insolubles
Content	54–56	14–16	1.5–2.5	27–29	8	2	5	1.5

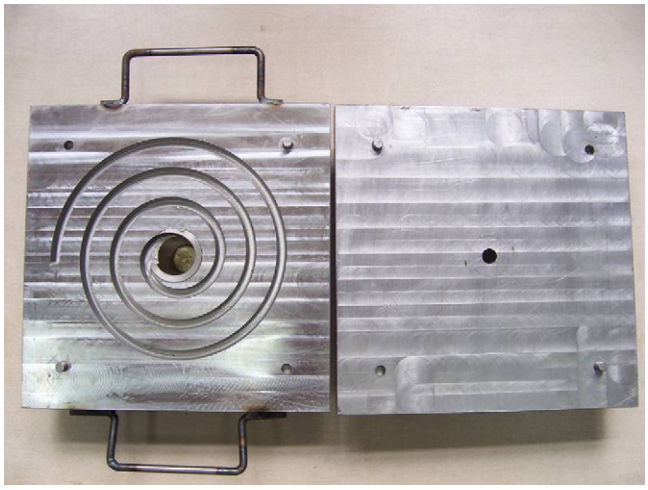

Fig. 1. Open mould showing as spiral-shaped permanent mould.

Table 2
Statistical volume fraction of inclusions in GW103K alloys with different treatments.

Refining flux	Number of fields	Average volume fraction
Unrefined	30	4.07%
Pure RJ6	30	2.84%
RJ6 + 5 wt.% YCl_3	30	0.87%

The size of specimens for immersion corrosion tests was 35 mm (diameter) × 4 mm (thickness). The specimens were polished on fine grades of emery papers up to 800 grit, and then immersed in a 5 wt.% NaCl aqueous solution at room temperature (25 ± 0.5 °C). After 3 days immersion, the specimens were cleaned by dipping in a solution of 15% Cr_2O_3 + 1% $AgNO_3$ in 500 ml water at boiling condition. The corrosion rates were obtained in weight loss per surface area and time (mg cm^{-2} d^{-1}).

Fluidity of the alloy was measured as the length of the metal flow in a spiral-shaped metallic mould (Fig. 1). The Archimedian spiral has a cross-section of 4 mm × 10 mm with a maximum running length of 1.4 m. In order to analyze the influence of nonmetallic inclusions on the fluidity of GW103K alloy, the pouring temperature was the same as casting condition (740 °C) and the mould preheating temperature was limited to 400 °C for the reason that higher mould temperatures promoted mould-metal reactivity and had a deleterious effect on surface finish.

Statistical volume fractions of nonmetallic inclusions in the alloy were measured with Leco image software. The purifying abilities of the fluxes were determined by comparing the volume fractions of nonmetallic inclusions before and after refining.

Table 3
Surface tensions of fluxes used in the experiments (760 °C).

Surface tension (N/m)	Fluxes	
	RJ6	RJ6 + 5 wt.% YCl_3
σ	0.212	0.195

The surface tensions of the fluxes were determined by RTW-05 Flux Properties admeasuring apparatus at 760 °C (refining temperature).

3. Results and discussion

3.1. Purifying effectiveness

It is necessary to clarify the main ingredients and morphologies of nonmetallic inclusions in alloy when we discuss the purifying effectiveness of different fluxes. Previous work [12] demonstrated that the largest inclusions in GW103K alloy exhibited spherical, bar-shape and irregular morphology. In addition to these large inclusions, some fine inclusions were dispersed within grains and on the grain boundary. The composition of these nonmetallic inclusions was analyzed by EDS as shown in Fig. 2. The results indicate that these nonmetallic inclusions are mainly MgO and oxides of Gd and Y.

Table 2 shows the statistical volume fractions of nonmetallic inclusions in the alloy. It is clear that the specimen refined by RJ6 + 5 wt.% YCl_3 additions exhibited the lowest average volume fraction (0.87%). The results indicate that the purifying effectiveness of RJ6 + 5 wt.% YCl_3 additions is better than that of pure RJ6 flux.

Generally, the procedure of flux removing nonmetallic inclusions from melts can be divided into three steps: first, the collision between nonmetallic inclusions and molten flux; second, the flux adsorbs nonmetallic inclusions; third, the inclusion and flux drop together down to the bottom of the crucible. The second step is the restrictive link of the three. The change of Gibbs free energy of refining process could be described as:

$$-\Delta G = [\sigma_{m-i} - (\sigma_{f-i} + \sigma_{m-f})]\ \Delta\omega \quad (1)$$

where σ_{m-i}, σ_{f-i} and σ_{m-f} are interface tensions between melt, inclusion and flux, respectively; $\Delta\omega$ is the increment of surface area.

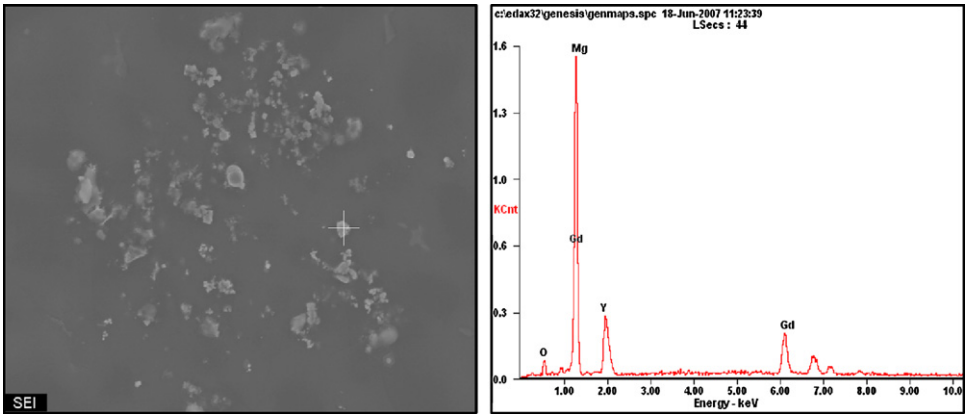

Fig. 2. SEM photographs and EDS analyses of nonmetallic inclusions in GW103K alloy.

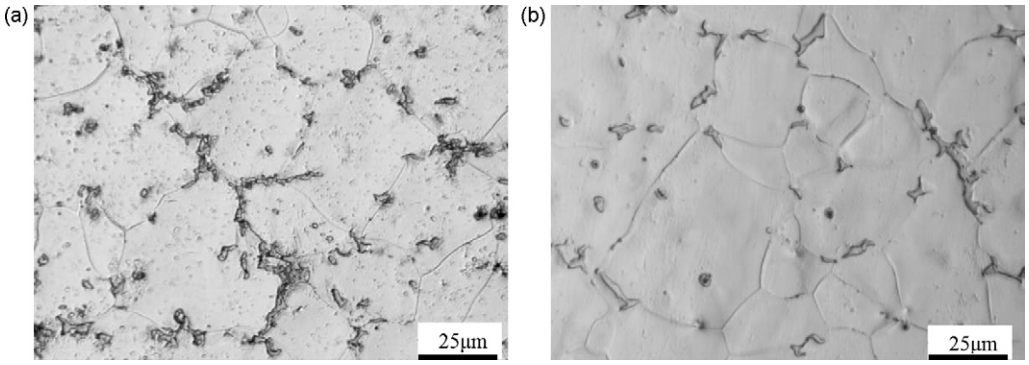

Fig. 3. Microstructures of GW103K alloy (as-cast condition) with different treatment conditions (a. unrefined, b. refined by RJ6 + 5 wt.% YCl_3 additions).

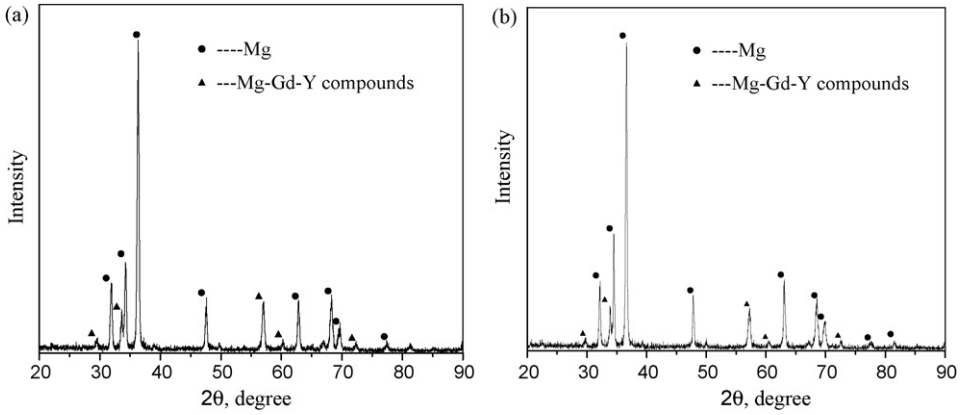

Fig. 4. X-ray diffraction (XRD) patterns of GW103K alloy with different treatment conditions (a. unrefined, b. refined by RJ6 + 5 wt.% YCl_3 additions).

As can be seen from Eq. (1), ΔG will be more negative with the decrease of σ_{m-f} and σ_{f-i}. The decrease of σ_{m-f} means that it is easy for nonmetallic inclusions to transfer from magnesium melt to the flux. Once the inclusions move to the surface of the molten flux, the low σ_{f-i} makes them be captured by flux easily.

As shown in Table 3, the surface tension of RJ6 + 5 wt.% YCl_3 additions is 0.195 N/m at 760 °C, which is lower than pure RJ6 flux (0.212 N/m). The low surface tension of the flux would decrease the interface tensions σ_{f-i} and then promotes the adsorption between flux and nonmetallic inclusion. Thus, the RJ6 + 5 wt.% YCl_3 additions exhibit better purifying effectiveness than pure RJ6 flux.

3.2. Microstructure

Fig. 3 shows the microstructures of GW103K alloy (as-cast) refined with RJ6 + 5 wt.% YCl_3 additions and pure RJ6 flux. For the specimens refined with RJ6 + 5 wt.% YCl_3 additions, it can be seen that the fraction of the inclusions is lower than in specimens refined by pure RJ6 flux. The phase compositions of GW103K alloy unrefined (Fig. 4a) and refined with RJ6 + 5 wt.% YCl_3 additions (Fig. 4b) were identified using XRD. The results indicate that the phase compositions of the alloy have not been changed after refining. It is still consisted of α-Mg and Mg–Gd–Y compounds. It could be concluded that the refining treatments almost have no influence on the microstructures of GW103K alloy.

In T6 condition, the microstructures are different from as-cast condition as shown in Fig. 5. All the eutectic phases dissolved into the matrix only with some inclusions and quadrate precipitates remained. The results indicate that the different refining processes still have no influence on the microstructure of the alloy under the condition of T6 heat treatment.

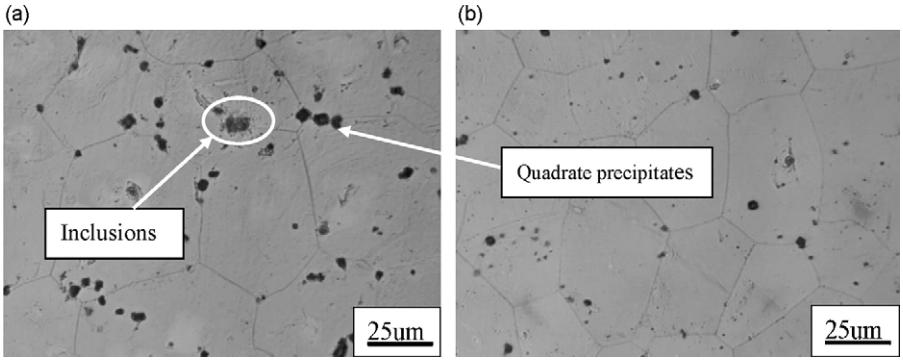

Fig. 5. Microstructures of GW103K alloy (T6 conditions) with different treatment conditions (a. unrefined, b. refined with RJ6 + 5 wt.% YCl_3 additions).

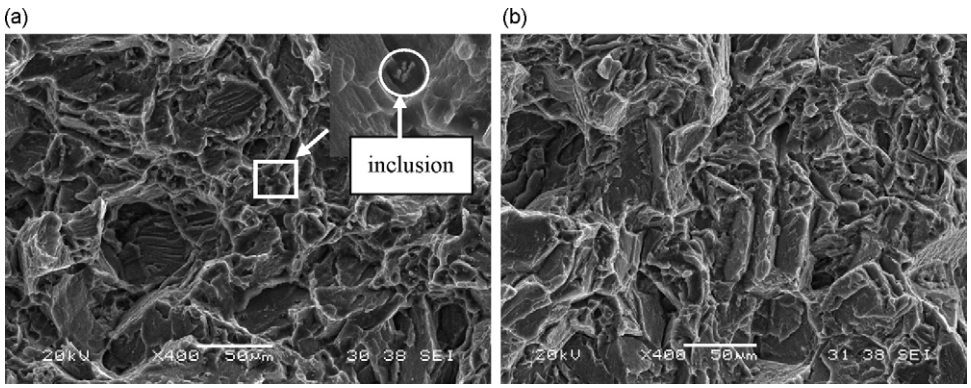

Fig. 6. Fractographs of tensile samples of GW103K alloy in as-cast condition (a. unrefined, b. refined by RJ6 + 5 wt.% YCl_3).

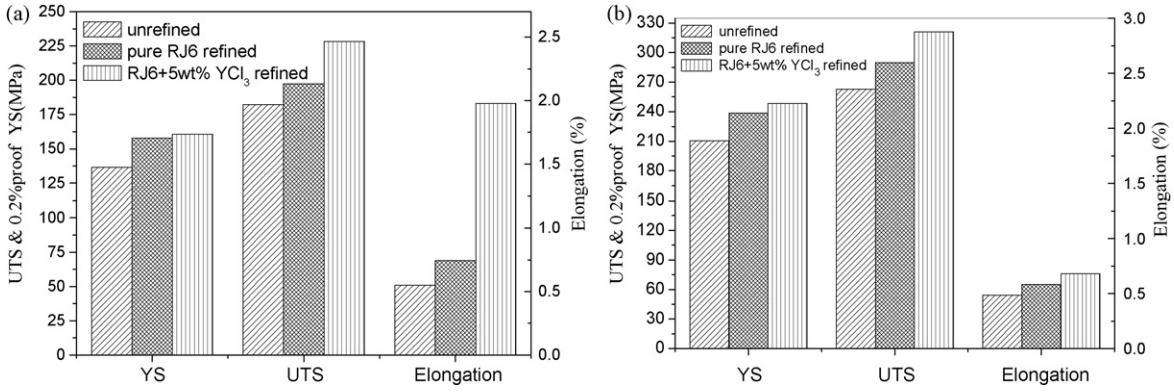

Fig. 7. Mechanical properties of GW103K alloy with different treatment conditions (a. as-cast, b. T6 condition).

The fracture surfaces of the specimens in as-cast condition after tensile tests are shown in Fig. 6. It is clear that the fracture patterns have not been changed by different refining processes. The fracture mechanisms are still quasi-cleavage crack. It should be noted that there are some nonmetallic inclusions (circled in Fig. 6a) on the fracture surface of unrefined specimen. For the specimen refined with RJ6 + 5 wt.% YCl_3 additions, however, the fracture surface is clean.

3.3. Mechanical properties

Fig. 7 shows the effects of different purification treatments on mechanical properties of GW103K alloy. In as-cast condition, compared with the specimens refined with pure RJ6 flux, the ultimate tensile strength (σ_b), 0.2% yield stress (σ_s) and elongation to failure (δ) of the specimens refined with RJ6 + 5 wt.% YCl_3 additions improved from 197.46 MPa, 157.67 MPa and 0.69% to 228.43 MPa, 160.76 MPa and 1.83%, respectively (Fig. 7a). Meanwhile, for the unrefined specimens, σ_b, σ_s and δ were only 182.25 MPa, 136.47 MPa and 0.51%, respectively. In T6 condition, the best combination of tensile properties was achieved with the 5 wt.% YCl_3 additions in flux. σ_b, σ_s and δ reached 320.91 MPa, 248.55 MPa and 0.78%, respectively.

Whether in as-cast or T6 condition, the best combination of mechanical properties of GW103K alloy could be obtained under the condition of RJ6 + 5 wt.% YCl_3 refining. Due to the deleterious effects of nonmetallic inclusions on inherent quality of the alloys, the improvement of the mechanical properties could be ascribed to the excellent ability of removing nonmetallic inclusions by RJ6 + 5 wt.% YCl_3 additions.

3.4. Corrosion resistance

The corrosion rates of the GW103K alloy treated with different refining processes are shown in Fig. 8. Whether in as-cast or T6 condition, the specimen refined with RJ6 + 5 wt.% YCl_3 additions exhibited the lowest corrosion rates. The corrosion resistance enhanced in the following sequence: unrefined < pure RJ6 < RJ6 + 5 wt.% YCl_3 additions. In as-cast condition, compared with specimens refined with pure RJ6 flux, the corrosion rate of the

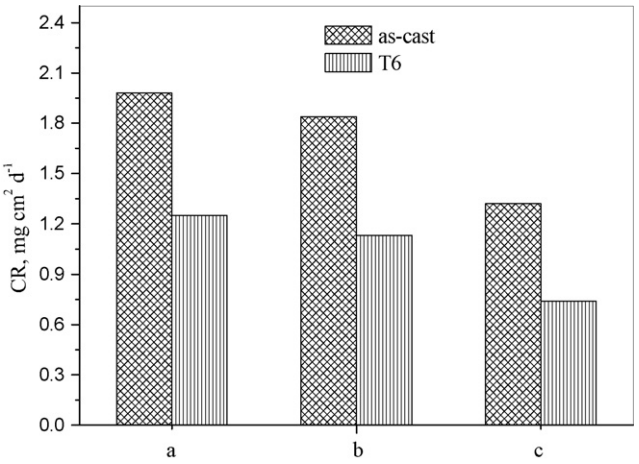

Fig. 8. Different treatments on the corrosion rates of GW103K alloy (a. unrefined, b. pure RJ6 refined, c. RJ6 + 5 wt.% YCl_3 refined).

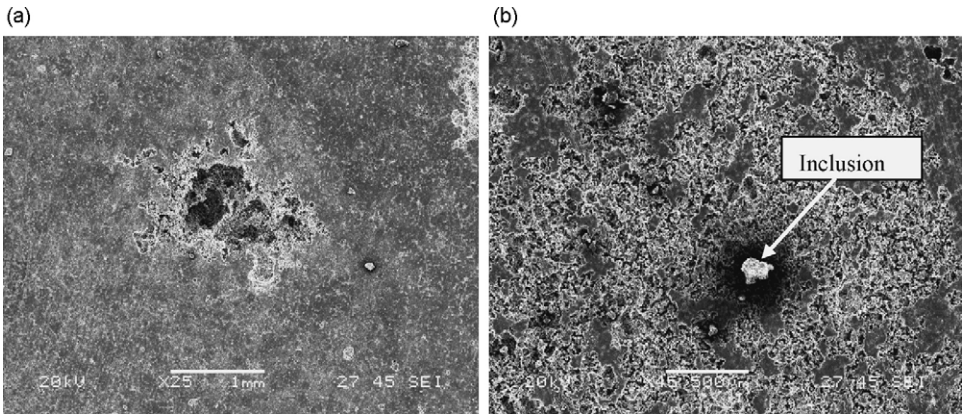

Fig. 9. Surface corrosion morphologies of GW103K alloy after immersed in 5 wt.% NaCl aqueous solution for 3 days (a. corrosion pit, b. corrosion morphology around nonmetallic inclusion).

specimens refined with RJ6 + 5 wt.% YCl_3 additions decreased from 1.84 to 1.32 mg cm^{-2} d^{-1}. For the specimens in T6 condition, the corrosion rates are generally lower than that of as-cast condition. This could be attributed to the change of phase compositions in the alloy. It could be found from Figs. 3 and 5 that the network eutectic phases in as-cast condition have dissolved into the α-Mg matrix after T6 heat treatment, only with some quadrate precipitates and nonmetallic inclusions remained. It is reported [13] that the eutectic phase acts as cathode and forms galvanic coupling corrosion with the Mg matrix when corrosion occurs, and then speeds up the corrosion process. Therefore, with the decreasing of the fraction of eutectic phase, the alloy in T6 condition exhibits better corrosion resistance than that in as-cast condition.

Fig. 9 shows the morphological characteristics of the corroded surfaces of the specimens immersed in 5 wt.% NaCl aqueous solution for 3 days. It can be seen that deep corrosion pits distributed on the surface of the unrefined specimens (Fig. 9a). Fig. 9b illustrates that the corrosion pit formed around the nonmetallic inclusion. Then, it could be assumed that corrosion started from the nonmetallic inclusions which were dispersed on the surface of the alloy. When corrosion extends to a certain degree, the nonmetallic inclusions desquamate from the surface and the corrosion pits come into being. Gao et al. [14] mentioned that the galvanic coupling could be formed between the nonmetallic inclusions and magnesium matrix during the course of corrosion and accelerated the corrosion process. Therefore, the reduction of nonmetallic inclusions decreases the cathode areas and thus improves the corrosion resistance of the alloy. It should be noted that the corrosion mechanism of nonmetallic inclusions is still not completely clear. Further research works are necessary to elucidate this mechanism.

3.5. Fluidity

It is clear from Table 4 that GW103K alloy melt refined with RJ6 + 5 wt.% YCl_3 has a much higher fluidity length (930 mm) than those unrefined (780 mm) and refined with pure RJ6 flux (828 mm). Taking into account the contents of nonmetallic inclusions in the alloy (as listed in Table 2), we can infer that the fluidity lengths will increase when the volume fractions of nonmetallic inclusions decreased.

Table 4
Relationship between flow length and different melt treatments.

Flow length	Refining methods		
	Unrefined	RJ6	RJ6 + 5 wt.% YCl_3
L_f (mm)	780	828	930

Ravi et al. [15] reported that the viscosity of the melt was an important parameter which greatly influenced the fluidity. Surappa and Rohatgi [16] observed that the increase in the viscosity of the melt due to dispersions of nonmetallic inclusions appeared to be one of the major reasons for the decrease of fluidity. For dilute suspensions (solid volume fraction, $\phi < 0.25$), the viscosity of the suspension can be estimated using Einstein's equation [17].

$$\mu_c = \mu_0[1 + 2.5\phi + 10.25\phi^2] \quad (2)$$

where μ_c is the apparent viscosity (g/cm s), μ_0 is the viscosity of fluids without any particle (g/cm s), and ϕ is the volume fraction of nonmetallic inclusions in the alloy melt. Eq. (2) indicates that the apparent viscosity rises markedly above the viscosity of pure melts when the volume fraction of nonmetallic inclusions increased. Based on the results listed in Table 2, it could be concluded that the viscosity of the alloy melt would decrease after refining with RJ6 + 5 wt.% YCl_3 additions. Obviously, this is helpful for improving the fluidity of the melt.

4. Conclusions

The effects of 5 wt.% YCl_3 additions in RJ6 flux on the mechanical, corrosion and fluidity properties of GW103K alloy were investigated and the following conclusions were made:

1. The addition of 5 wt.% YCl_3 into RJ6 flux decreased the surface tension of the flux, which is one of the important parameters to improve the purification effectiveness of the flux.
2. The mechanical properties of GW103K alloy both in as-cast and T6 conditions were greatly enhanced by RJ6 + 5 wt.% YCl_3 additions. The ultimate tensile strength, yield stress and elongation reached the maximum value of 228.43 MPa, 160.76 MPa and 1.83% for as-cast condition, and 320.91 MPa, 248.55 MPa and 0.78% for T6 condition.
3. The corrosion rate of the alloy refined by RJ6 + 5 wt.% YCl_3 declined to the minimal 1.32 mg cm^{-2} d^{-1} for as-cast specimens.
4. The fluidity of GW103K alloy melt refined with RJ6 + 5 wt.% YCl_3 additions were greatly improved due to the decrease of viscosity.

Acknowledgements

This work was funded by the National Basic Research Program of China (No. 2007CB613701), National Key Technology R&D Program of China (No. 2006BAE04B07-2) and Program of Shanghai Subject Chief Scientist (No. 08XD14020). The authors also would like to thank the Center of Analysis and Measurement of Shang-

hai Jiao Tong University for assistance with the XRD and the Field Emission Scanning Electron Microscope (FE-SEM).

References

[1] S.M. He, X.Q. Zeng, L.M. Peng, X. Gao, J.F. Nie, W.J. Ding, J. Alloys Compd. 427 (2007) 316–323.
[2] S.M. He, X.Q. Zeng, L.M. Peng, J. Alloys Compd. 421 (2006) 309–313.
[3] B. Smola, I. Stulíková, F. Von Buch, B.L. Mordike, Mater. Sci. Eng. A 324 (2002) 113–117.
[4] I. Anthony, S. Kamado, Y. Kojima, Mater. Trans. 42 (2001) 1206–1211.
[5] I. Anthony, S. Kamado, Y. Kojima, Mater. Trans. 42 (2001) 1212–1218.
[6] P. Vostrý, B. Smola, I. Stulíková, F. Von Buch, B.L. Mordike, Phys. Stat. Sol. A 175 (1999) 491–500.
[7] B.L. Mordike, T. Ebert, Mater. Sci. Eng. A 302 (2001) 37–45.
[8] I. Shigeru, N. Yuji, K. Shigeharu, J. Jpn. Inst. Light Met. 44 (1994) 3–8.
[9] W.B. Du, Y.F. Wu, Z.R. Nie, X.K. Su, T.Y. Zuo, Rare Met. Mater. Eng. 35 (2006) 1345–1348.
[10] H.T. Gao, G.H. Wu, W.J. Ding, Y.P. Zhu, Trans. Nonferrous Met. Soc. China 14 (2004) 530–536.
[11] Z.H. Cheng, Magnesium Alloy, Chemical Industry Press, Beijing, 2004, pp. 64–70.
[12] W. Wang, G. Wu, Q. Wang, Y. Huang, W. Ding, Mater. Sci. Eng. A (2008), doi:10.1016/j.msea.2008.12.004.
[13] X.W. Guo, J.W. Chang, S.M. He, W.J. Ding, Electrochim. Acta 52 (2007) 2570–2579.
[14] H.T. Gao, G.H. Wu, W.J. Ding, L.F. Liu, X.Q. Zeng, Y.P. Zhu, Mater. Sci. Eng. A 368 (2004) 311–317.
[15] K.R. Ravi, R.M. Pillai, K.R. Amaranathan, B.C. Pai, M. Chakraborty, J. Alloys Compd. 456 (2008) 201–210.
[16] M.K. Surappa, P.K. Rohatgi, Metall. Trans. B 12B (1981) 327–332.
[17] A. Einstein, Ann. Phys. 34 (1911) 591.